

DOI: 10.5281/zenodo.3784341
CZU 621.373.8



CHARACTERISTICS OF QUANTUM DOTS LASER SUBJECTED TO CONVENTIONAL AND FILTERED OPTICAL FEEDBACK

Spiridon Rusu, ORCID ID: 0000-0002-7845-0103, Tatiana Oloinic,
Vitalie Chistol, ORCID ID: 0000-0002-4761-5892,
Vasile Tronciu*, ORCID: 0000-0002-9164-2249

Department of Physics, Technical University of Moldova, 168, Stefan cel Mare Bd., Chisinau, Moldova

*Corresponding author: Vasile Tronciu, vasile.tronciu@fiz.utm.md

Received: 03.22.2020

Accepted: 05.05.2020

Abstract. The quantum dots laser under the influence of conventional and filtered feedback is analyzed in the framework of the extended Lang-Kobayashi rate equations. The feedbacks comes from two separate branches: conventional and filtered optical feedback. We introduce a filtered feedback to control the unstable behavior of laser induced by conventional optical feedback. The stationary states, so called external filtered modes, of quantum dot laser under the influence of double feedback are obtained analytically. The locations of these modes are plotted in the plane of different parameters. Finally, it is shown that under appropriate conditions the laser system generate different behavior as continuous wave, periodic and chaotic behavior. In the case of equal feedback strengths in both channels it is shown that for a small feedback strength the phase portrait is a stable focus. With increase of the both feedback strengths the phase portrait became a limit cycle, and finally goes to a strange attractor.

Keywords: *conventional and filtered optical feedback, externally cavity modes, quantum dots lasers, rate equations, stationary states, stable focus, limit cycle, strange attractor.*

1. Introduction

During recent years the control of semiconductor laser showing dynamical instabilities has received considerable attention due to its fundamental importance and practical applications. It is well known that laser under influence of conventional optical feedback shows different behaviors e.g. periodic, quasi-periodic or chaotic oscillations. Such chaotic behavior is benefic in applications like chaos-based communications [1, 2]. On the other hand, such oscillations are unwanted in many applications. Thus, the control of laser emission become the subject of different investigations. Ott, Grebogi and Yorke [3] show that a chaotic attractor can be stabilized by a little amount time dependent perturbation and transformed into periodic motion. Later on improving of this method in different fields have been reported [4-6]. Theoretical and experimental method of feedback control was proposed in 1991 by Signer et all [7]. Pyragas suggested time-continuous self-controlling feedback method for stabilization of the unstable periodic orbits [8, 9]. A study of the

continuous-wave operation of a semiconductor laser subject to an external optical feedback from a Fabry-Perot resonator in a case where the emission is resonant to a reflection minimum of the resonator was reported in [10]. Such configuration was treated in the framework of Lang-Kobayashi equations by finding the nature of bifurcations and the stability of steady state solutions. It was shown that in contrast to conventional optical feedback from a single mirror, the locus of external cavity modes is not elliptic but represents a tilted eight with possible satellite bubbles. The results obtained in [10] are a prototype for all-optical realizations of delayed feedback control. Advantages of controlling the unstable dynamics of a quantum wells semiconductor laser subject to conventional optical feedback by means of a second filtered feedback branch is presented in [11]. There were obtained analytical solutions of the double cavity feedback and has shown numerically that the region of stabilization is much larger when using a second branch with filtered feedback than when using a conventional feedback one.

It is well known that the quantum dots (QDs) become the main element for lasers. The advantages of QDs lasers were predicted some twenty years ago and include low threshold current, weak temperature dependence, increased material and differential gain, high modulation frequency, low jitter under pulsed operation, low chirp and low sensitivity to optical feedback [12 - 15]. Although QDs lasers are now generally better than quantum well lasers, the characteristics of QDs lasers still deviate from the ideal case due to a number of unforeseen phenomena, including the thermal population of excited dot and barrier states, the loss of carriers to non-radiative centers and the presence of inhomogeneous broadening due to non-uniformities. Even a small amount of feedback can destabilize lasers, inducing instabilities and resulting in very complicated dynamical behavior – so called chaos. In the case of communication, CD and DVD systems, the feedback is due to reflection from interconnection or from CD and can cause an increase in phase and intensity noise, mode-hopping, coherence collapse and linewidth broadening. The present paper represents a first theoretical study of a configuration of double feedback conventional and filtered for lasers with active region quantum dots. The paper is structured as follows. We start in Section 2 by describing the setup of QDs laser under the influence of double feedbacks. We introduce also in this Section an appropriate model to describe this setup. Section 3 presents a study of the stationary states a laser under the influence of T-type cavity feedback: one being conventional and second filtered. The suitable conditions for the different laser system behavior were obtained. Finally, conclusions are given in Section 4.

2. Setup and model

The proposed setup is depicted schematically in Figure 1. It consists of a quantum dots laser with external feedbacks from reflectors R_1 and R_2 . One feedback branch, of reflectivity R_1 , is so called conventional optical feedback and the other governed by R_2 is the filtered feedback.

For simplicity, we assume single reflection in both branches. We assume a grating filter described by a response function $r(\omega)$, expressed by a Lorentzian function [16]

$$r(\omega) = \frac{\lambda}{\lambda + i(\Delta\omega - \omega)}, \quad (1)$$

where λ is a central frequency, $\Delta\omega$ is the detuning with respect to the solitary laser frequency ω_0

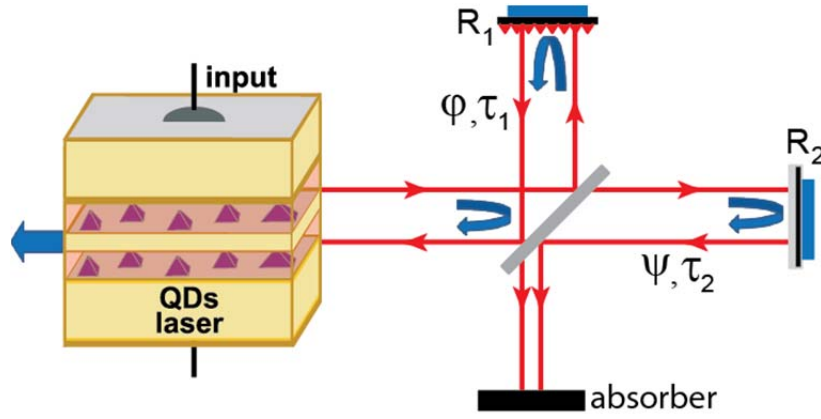


Figure 1. The schematic view of the setup.

The dynamics of quantum dots laser with double feedbacks is analyzed in the framework of the extended Lang-Kobayashi rate equations

$$\frac{dE}{dt} = \frac{1}{2}(1+i\alpha)\left[-\gamma_{np} + g(2\rho-1)\right]E(t) + \Gamma_1 e^{i\varphi} E(t-\tau_1) + \Gamma_2 F(t), \quad (2)$$

$$\frac{dF}{dt} = \Lambda E(t-\tau_2) e^{i\psi} + (i\Delta\omega - \Lambda)F(t), \quad (3)$$

$$\frac{d\rho}{dt} = -\gamma_{ns}\rho - (2\rho-1)|E|^2 + (CN^2 + BN)(1-\rho), \quad (4)$$

$$\frac{dN}{dt} = J - N - 2(CN^2 + BN)(1-\rho), \quad (5)$$

where $E(t)$ and $F(t)$ are the complex field amplitudes, $\rho(t)$ is the occupation probability in the quantum dot, and $N(t)$ excess carrier density. The following parameter values are used for the calculated results. Henry factor $\alpha = 2$, and $\tau_1 = 0.3$, $\tau_2 = 0.2$ the external cavity round trip times. $g = 1200$ is the differential gain, and $J = 20$ is pumping parameter. The constants $B = 0.012$ and $C = 40$ describe the transport of charge carriers through carrier-phonon interaction, $\gamma_{ns} = 1.0$, and $\gamma_{np} = 500$.

3. Stationary states. Numerical results.

The stationary states of the system of equations (2) – (5) are given by rotating wave solutions so called external cavity modes (ECMs) of the following form

$$E = E_s e^{i\omega_s t}; \quad F = F_s e^{i\omega_s t + i\Phi_s}; \quad \rho = \rho_s; \quad N = N_s. \quad (6)$$

Inserting Eq. (6) into Equations (2) – (5) we obtain the following equations for E_s, F_s, ρ_s, N_s :

$$\frac{dE_s}{dt} = -i\omega_s E_s(t) + \frac{1}{2}(1+i\alpha)\left[-\gamma_{np} + g(2\rho_s-1)\right]E_s(t) + \Gamma_1 E_s(t-\tau_1) e^{-i(\omega_s \tau_1 - \varphi)} + \Gamma_2 F_s(t) e^{i\Phi_s}, \quad (7)$$

$$\frac{dF_s}{dt} = -i\omega_s F_s + \Lambda E_s(t-\tau_2) e^{-i(\omega_s \tau_2 + \Phi_s - \psi)} + (i\Delta\omega - \Lambda)F_s(t), \quad (8)$$

$$\frac{d\rho_s}{dt} = -\gamma_{ns}\rho_s - (2\rho_s-1)|E_s|^2 + (CN_s^2 + BN_s)(1-\rho_s), \quad (9)$$

$$\frac{dN_s}{dt} = J - N_s - 2(CN_s^2 + BN_s)(1 - \rho_s). \quad (10)$$

In what follows we consider the derivatives of the left side of Equations (7) – (10) equal to zero. Thus, we obtain

$$i\omega_s E_s = \frac{1}{2}(1 + i\alpha)[- \gamma_{np} + g(2\rho_s - 1)]E_s + \Gamma_1 E_s e^{-i(\omega_s \tau_1 - \varphi)} + \Gamma_2 F_s e^{i\Phi_s}, \quad (11)$$

$$i\omega_s F_s = (i\Delta\omega - \Lambda)F_s + \Lambda E_s e^{-i(\omega_s \tau_2 + \Phi_s - \psi)}, \quad (12)$$

$$\gamma_{ns} \rho_s = (CN_s^2 + BN_s)(1 - \rho_s) - (2\rho_s - 1)|E_s|^2, \quad (13)$$

$$J = N_s + 2(CN_s^2 + BN_s)(1 - \rho_s). \quad (14)$$

After some transformations, we obtain a transcendental equation for ω_s

$$\omega_s = -\Gamma_1 [\alpha \cos(\omega_s \tau_1 - \varphi) + \sin(\omega_s \tau_1 - \varphi)] - \Gamma_2 \frac{F_s}{E_s} (\alpha \cos \Phi_s - \sin \Phi_s), \quad (15)$$

and the following equations for ρ_s , N_s and E_s :

$$\rho_s = \frac{1}{2g} \left[g + \gamma_{np} - 2\Gamma_1 \cos(\omega_s \tau_1 - \varphi) - 2\Gamma_2 \frac{F_s}{E_s} \cos \Phi_s \right], \quad (16)$$

$$N_s = \frac{-[2B(1 - \rho_s) + 1] + \sqrt{[2B(1 - \rho_s) + 1]^2 + 8C(1 - \rho_s)J}}{4C(1 - \rho_s)}, \quad (17)$$

$$E_s = \sqrt{\frac{J - N_s - 2\gamma_{ns} \rho_s}{2(2\rho_s - 1)}}, \quad (18)$$

with

$$\frac{F_s}{E_s} = \cos \left[\arctg \frac{\omega_s - \Delta\omega}{\Lambda} \right], \quad (19)$$

$$\Phi_s = \psi - \omega_s \tau_2 - \arctg \frac{\omega_s - \Delta\omega}{\Lambda}. \quad (20)$$

In what follows we take into account the complexity of amplitudes $E_s = E_1 + iE_2$; $F_s = F_1 + iF_2$. From Equations (7) - (10) we obtain

$$\begin{aligned} \frac{dE_1}{dt} = & \omega_s E_2 + \frac{1}{2}[-\gamma_{np} + g(2\rho_s - 1)](E_1 - \alpha E_2) + \Gamma_1 [E_1(t - \tau_1) \cos(\omega_s \tau_1 - \varphi) + \\ & + E_2(t - \tau_1) \sin(\omega_s \tau_1 - \varphi)] + \Gamma_2 (F_1 \cos \Phi_s - F_2 \sin \Phi_s), \end{aligned} \quad (21)$$

$$\begin{aligned} \frac{dE_2}{dt} = & -\omega_s E_1 + \frac{1}{2}[-\gamma_{np} + g(2\rho_s - 1)](\alpha E_1 + E_2) + \Gamma_1 [E_2(t - \tau_1) \cos(\omega_s \tau_1 - \varphi) - \\ & - E_1(t - \tau_1) \sin(\omega_s \tau_1 - \varphi)] + \Gamma_2 (F_2 \cos \Phi_s + F_1 \sin \Phi_s), \end{aligned} \quad (22)$$

$$\frac{dF_1}{dt} = \omega_s F_2 - \Delta \omega F_2 - \Lambda F_1 + \Lambda [E_1(t - \tau_2) \cos(\omega_s \tau_2 + \Phi_s - \psi) + E_2(t - \tau_2) \sin(\omega_s \tau_2 + \Phi_s - \psi)], \quad (23)$$

$$\frac{dF_2}{dt} = -\omega_s F_1 + \Delta \omega F_1 - \Lambda F_2 + \Lambda [E_2(t - \tau_2) \cos(\omega_s \tau_2 + \Phi_s - \psi) - E_1(t - \tau_2) \sin(\omega_s \tau_2 + \Phi_s - \psi)], \quad (24)$$

$$\frac{d\rho_s}{dt} = -\gamma_{ns} \rho_s - (2\rho_s - 1)(E_1^2 + E_2^2) + (CN_s^2 + BN_s)(1 - \rho_s), \quad (25)$$

$$\frac{dN_s}{dt} = J - N_s - 2(CN_s^2 + BN_s)(1 - \rho_s). \quad (26)$$

For different values of parameters, the Equations (15) – (20) have different number of roots ω_s . Let us first consider the case of only conventional optical feedback. In this case the solutions are located on top of an ellipse in the plane (N_s, ω_s) . Figure 2 shows the location of ECMs for different values of feedback strength. As one can see the ellipses increase when the feedback strength increases.

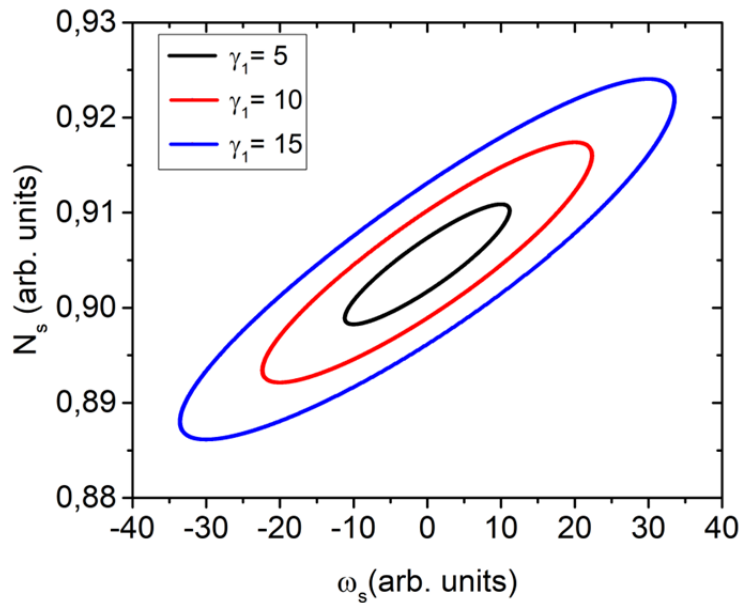


Figure 2. External cavity modes in the plane of $(N_s - \omega_s)$ for different values of feedback strength in conventional feedback branch. The feedback in filtered branch is absent.

When the filtered feedback is added the locations of the external cavity modes and the general picture become more complicated. A narrow filter with $\Lambda = 1$ GHz is considered in this paper.

The detuning $\Delta\omega$ is chosen to be equal to zero. Figure 3 shows the location of modes for different feedback strength in filtered feedback branch. For $\gamma_2 = 0$ the modes, as was mentioned above, are located on the ellipse (see Figure 3a). When γ_2 is increased to 5 the ellipse is deformed as shown in Figure 3b. A further deformation of ellipse is observed for $\gamma_2 = 10$. A further increase of γ_2 leads to apparition of double bubbles (see Figure 3d). Thus, with help of second branch we can control the stationary states of external cavity modes.

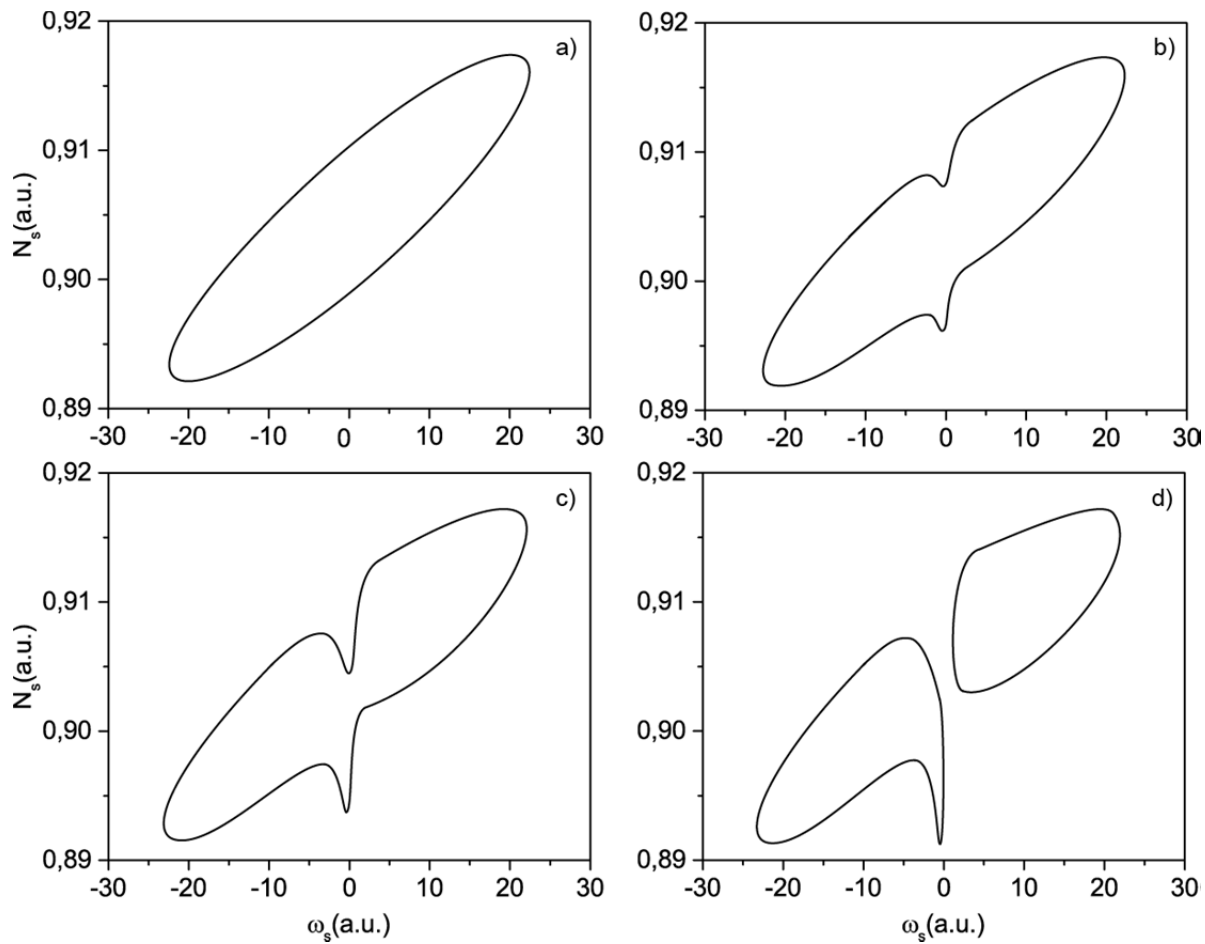


Figure 3. The location of external cavity modes for a fixed value of feedback strength of conventional optical feedback ($\gamma_1 = 10$) and different values of feedback strength in filtered brunch: a) $\gamma_2 = 0$, b) $\gamma_2 = 5$, c) $\gamma_2 = 10$, d) $\gamma_2 = 15$.

In what follows, we investigate the evolution in time of the laser system by using the equations (21) – (26). Figure 4 shows the results of numerical integration by Runge-Kutta method of the system (21) – (26). We consider the case of equal feedback strengths in both channels.

Left panels in Figure 4 show the pulse traces of external output power. In the center panels, we show the phase portraits in the plane of two parameters (optical power P – carrier density N). The right panels shows the power spectra. Figure 4a shows these dependences for $\gamma_1 = \gamma_2 = 15$. One can see the relaxation oscillation of few nanoseconds with the phase portrait of stable focus. When the feedback strengths are increased to $\gamma_1 = \gamma_2 = 20$ the pulse-trace become periodic and the phase portrait is a limit cycle. A dominant mode is present in the right panel of Figure 4b.

A further increase of both feedback strengths to $\gamma_1 = \gamma_2 = 40$ leads to the appearance of chaotic behavior in the pulse trace (see left panel of Figure 4c).

The phase portrait (center panel) is strange attractor.

The chaotic behavior is confirmed by wide power spectra shown in right panel of Figure 4c.

Thus, the double cavity feedback imply the different behavior of system from continuous operation to chaos.

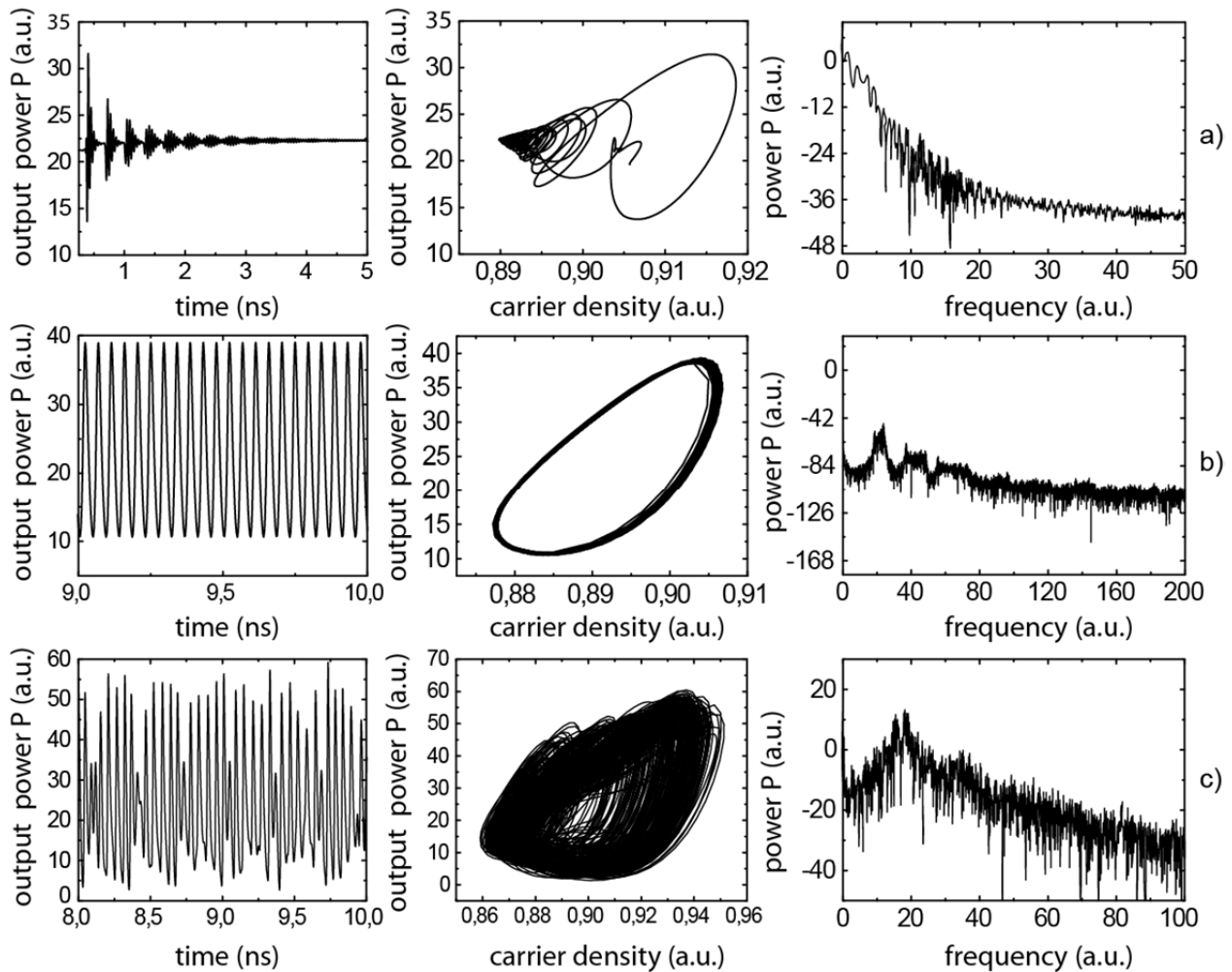


Figure 4. A typical optical power time trace (left), phase portrait (center) and the power spectrum (right) of a semiconductor laser is shown in Figure 1 for: a) $\gamma_1 = \gamma_2 = 15$, b) $\gamma_1 = \gamma_2 = 20$, c) $\gamma_1 = \gamma_2 = 40$.

4. Conclusions

We have treated in this paper a quantum dots laser under the influence of conventional and filtered feedback in the framework of properly adapted Lang-Kobayashi method.

We obtain analytical solutions for stationary states, so called externally cavity modes. It is shown that in case of only conventional optical feedback these steady states are located on top of an ellipse in the $(N_s - \omega_s)$ plane. In case of the double cavity feedback (conventional and filtered) the ellipse is strongly distorted and breaks into several bubbles. The results presented in this paper show that under appropriate conditions the laser system is capable to generate different behavior as continuous wave, periodic and robust chaotic behavior. We believe that our work provides a good basis for future study and, in particular, provides some pointers for more detailed investigations of quantum dots lasers dynamics under the influence of conventional and filtered feedback.

Acknowledgments. The authors acknowledge financial support from state project 20.80009.5007.08.

References

1. Argyris A., Syvridis D., Larger L., Annovazzi-Lodi V., Colet P., Fischer I., García-Ojalvo J., Mirasso C.R., Pesquera L., Shore K.A. Chaos-based communications at high bit rates using commercial fibre-optic links. In: *Nature*, 2005, 438, pp. 343-346.
2. Tronciu V.Z., Miraso C.R., Colet P., Hamacher M., Benedetti M., Vercesi V., Annovazzi-Lodi V. Chaos generation and synchronization using an integrated source with an air gap. In: *IEEE Journal of Quantum Electronics*, 2010, 46, pp.1840-1846.
3. Ott E., Grebogi C., Yorke J.A. Controlling chaos. In: *Physical Review Letters*, 1990, 64(11), pp. 1196-1199.
4. Roy R., Murphy T.W., Maier T.D., Gills Z., Hunt E.R. Dynamical control of a chaotic laser: Experimental stabilization of a globally coupled system. In: *Physical Review Letters*, 1992, 68(9), pp.1259-1262.
5. Garfinkel A., Spano M.L., Ditto W.L., Weiss J.N. Controlling cardiac chaos, In: *Science*, 1992, 257, pp. 1230-1235.
6. Dressler U., Nitsche G. Controlling chaos using time delay coordinates. In: *Physical Review Letters*, 1992, 68(1), pp.1-4.
7. Singer J., Wang Y.Z., Bau H.H. Controlling a chaotic system. In: *Physical Review Letters*, 1992, 66(9), pp.1123-1125.
8. Pyragas K. Continuous control of chaos by self-controlling feedback. In: *Physics Letters A*, 1992, 170(6), pp.421-428.
9. Pyragas K. Stabilization of unstable periodic and aperiodic orbits of chaotic systems by self-controlling feedback. In: *Zeitschrift für Naturforschung A*, 1993, 48(5-6), pp.629-632.
10. Tronciu V.Z., Wünsche H.-J., Wolfrum M., Radziunas M. Semiconductor laser under resonant feedback from a Fabry-Perot resonator: Stability of continuous-wave operation. In: *Physical Review E*, 2006, 73(4), id. 046205. <https://journals.aps.org/pre/abstract/10.1103/PhysRevE.73.046205>.
11. Ermakov I.V., Tronciu V.Z., Colet P., Mirasso C.R. Controlling the unstable emission of a semiconductor laser subject to conventional optical feedback with a filtered feedback branch. In: *Optics Express*, 2009, 17(11), pp.8749-8755.
12. Arakawa Y., Sakaki H. Multidimensional quantum well laser and temperature dependence of its threshold current. In: *Applied Physics Letters*, 1982, 40, pp.939-941.
13. Saito H., Nishi K., Kamei A., Sugou S. Low chirp observed in directly modulated quantum dot lasers. In: *IEEE Photonics Technology Letters*, 2000, 12, pp.1298-1300.
14. Grundmann M. The present status of quantum dot lasers. In: *Physica E: Low-dimensional Systems and Nanostructures*, 1999, 5(3), pp.167-184.
15. Bimberg D., Ribbat C. Quantum dots: lasers and amplifiers. In: *Microelectronics Journal*, 2003, 34, pp. 323-328.
16. Weisstein E.W. "Lorentzian Function." From *MathWorld* -- A Wolfram Web Resource., <http://mathworld.wolfram.com/LorentzianFunction.html>.